**Wiesław Barnat,
Dariusz Sokołowski,
Roman Gieleta,
Paweł Bogusz**

Numerical and Experimental Studies of Material Properties of Special - Purpose Material Twaron T750

DOI: 10.5604/12363666.1152720

**Military University of Technology,
Faculty of Mechanical Engineering,
Department of Mechanics
and Applied Computer Science,**
Warsaw, Poland,
E-mail: wbarnat@wat.edu.pl,
dsokolowski@wat.edu.pl,
rgieleta@wat.edu.pl,
pbogusz@wat.edu.pl

Abstract
The subject of this paper is an attempt to define the fundamental constants of materials for special-purpose material - aramid dry faricTwaronT750. During research on this problem, tensile tests of dry fabric TwaronT750 were made on an Istron 8802 strength testing machine. The test was filmed with a Phantom V12 high-speed camera. A numerical model of the fabric architecture was made using commercial HyperMesh and LS-DYNA software. In the numerical model a whole research area was represented.

Key words: *dry aramid fabric, mechanical properties, finite element analysis.*

Introduction

Technological progress in the field of manufacturing of new materials, and especially the increasing demand for them, cause that in recent times the increasing use of materials with a collective name of material for special purposes has been observed. These materials are characterised by heightened physical properties. For a long time, because of their high cost, these materials could be found only in industries of high technology, such as space flight and military applications (especially in aviation). Technological progress that has been made in the past few decades has reduced the unit costs of these materials, which has resulted in the greater availability of them.

Fibrous materials in the form of fabrics have been known by mankind for thousands of years. However, fibrous structural materials appeared in use at the beginning of the previous century. The rapid development of these materials began during the Second World War and after it. It is connected with the dynamic development of the aviation industry. Most fibrous structural materials in the industry are combined with different types of resins. However, some applications are independent (for example in terms of protection against bullets or fragments). Because of their anisotropy and nonlinear behaviour, fabrics are interesting material, which is illustrated in papers by [1 - 3]. The impact of the architecture of fabric on the kinetic energy dissipation is not trifling, as is ilustrated in the work [4]. To understand how fabric works as a geometrical construction, the micromechanics of the fibrous material cannot be omitted [5].

In this paper the problem of the numerical modeling of aramid dry fabric Twaron T750 has been raised. This fabric is a special-purpose material used in the manufacture of bulletproof vests. Twaron T750 fabric is characterised by a high dense weave. In order to achieve a reliable model of the real fabric, a simple tensile test of six samples made of Twaron T750 fabric was done. These studies were used to establish a numerical model as precise as possible by means of commercial software - LS-DYNA.

The rapid development of computational techniques has allowed a more detailed description of the structures of dry fabrics. Yet, in the not so distant past, dry fabric in the bullet impact test was modelled in the form of an averaged material continuum which was built using membrane or shell elements. With the arrival of more and more powerful computational units on the market, there have appeared options for modelling of architecture fabric weave and bundle thickness. This kind of modeling allows to grasp the phenomena of contact between bundles in roving, enabling to represent the phenomena of movement between bundles. In the literature there are three ways of modeling roving bundles in the fabric architecture. The first way is to model the bundles in the form of flat elements (with specified thickness, so called. 2D) [6]. The second approach is to model the bundles using three-dimensional elements [7 - 10]. The third way is to model by hybrid modeling using the two methods above, as presented by Nilakantan [8 - 10]. The most cost-effective computational method is, of course, the use of 2D components. This type of analysis is used in cases where the fabric is loaded in the plane. Despite the large approximations, this kind of modeling is fully effective and efficient. In this paper, the problem of modeling special fabrics will be considered using 2D elements. 3D modeling of roving bundles should be used to model a fabric loaded perpendicular to the plane, making models very expensive computationally. So far, in the modeling of bundles, authors such as Nilakantan or Barauskas have used

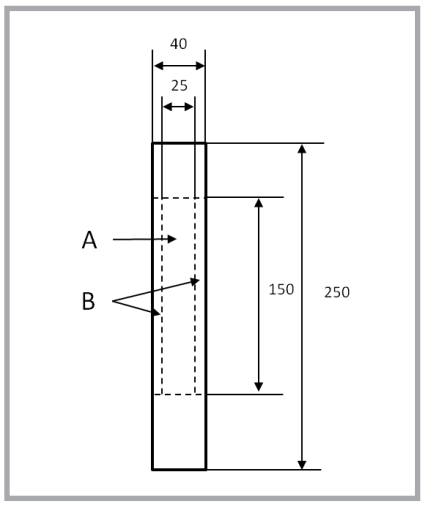

Figure 1. *Schema of sample, A - research area, B - area where the roving bundles in the direction of the samples were removed.*

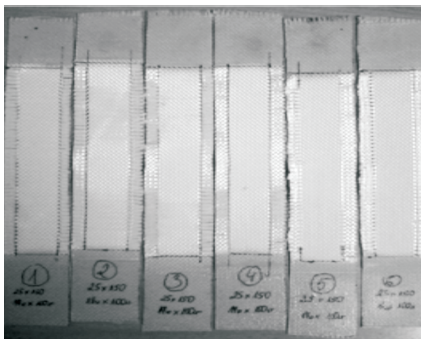

Figure 2. *Samples of fabric made from Twaron T750.*

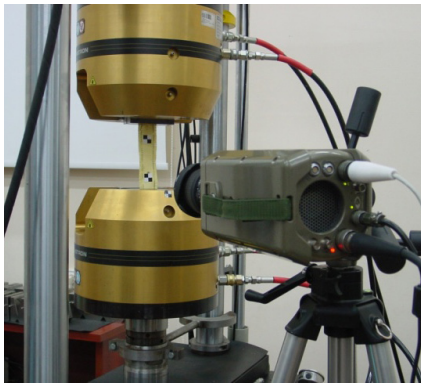

Figure 3. *Sample clamped in the Istron 8802 testing machine, filmed by a Phantom V12 high-speed camera.*

two 3D elements for the thickness of the bundle, which in the modelling of other phenomena is rather not acceptable.

In the literature available there is a lack of examples for the validation of numerical models with experimentation in case studies for dry fabrics. This article will be presented a validation of the numerical model for Twaron T750 fabric with experimental results.

Experimental tests

Coupon preparation process for aramid fabric

The basic test, as far as possible, thoroughly examining the properties of dry fabric, is the plane tensile test. The main phenomenon that the authors wanted to capture was, primarily, a way to straighten roving bundles and the impact of this phenomenon on the force curve characteristics, as a function of the displacement. Another important parameter obtained from the validation studies was the maximum force at the time of destruction (break) of the sample and the displacement at which the sample broke.

Figure 1 shows a sample that was proposed for a simple tensile test. The measurement part of the sample (dry fabric) in ***Figure 1,*** marked with the letter "A", has dimensions 150 mm × 25 mm, giving a ratio of 6:1, which allows to assume that the principle of de Saint-Venant was met in the test. The area shown in ***Figure 1*** marked with the letter "B" is that where roving bundles were removed in the direction of the sample. Bundles across the sample were left in order to prevent drawing them into the test area during the straightening of bundles along the sample. The overall dimensions of the samples were 250 × 40 mm.

In order to evaluate the results, 6 samples of Twaron T750 fabric were tested. Samples were made at the Laboratory Lamination Department of Mechanics and Applied Computer Science MUT. ***Figure 2*** shows samples ready for testing. Besides the dimensions of samples, the number of bundles in the direction of the sample were marked: 17 ± 1 and 100 ± 5. These values are very important in the numerical modeling problem described.

Test results

Simple tensile tests were done at the KMiIS MUT laboratory on an Istron 8802 machine - ***Figure 3***. The tests were filmed with a Phantom V12 high-speed camera at a frequency of 10000 – in frames/s. The Piston machine speed was set to 50 in mm/s.

Figure 4, shows pictures from the high-speed camera in four moments of time: the start of the test, at the time of breaking of the first fibres (for time 183.4 ms), the exact time at which the sample broke

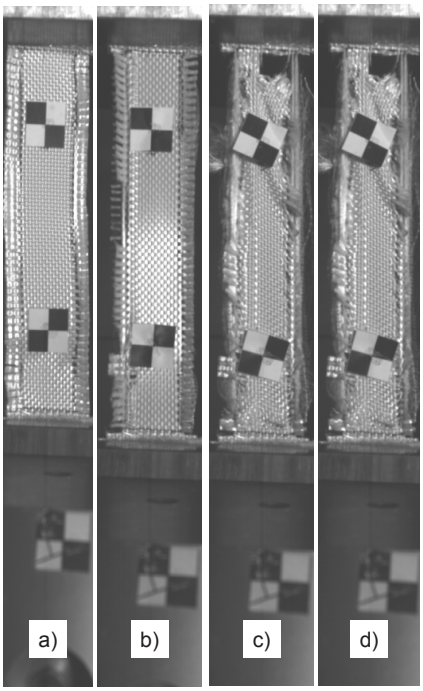

Figure 4. *Pictures of sample X: a) undeformed sample, b) first bundles broken, c) exact time at which sample was broken, d) completely destroyed sample.*

(for time 193.4 ms) and totally broke (for time 318.6 ms).

Figure 4 illustrates the method of recording deformation together with that in the final stage of destruction of the sample made from aramid fibres.

In the first stage (***Figure 4.a***) of the test, pre-tension of the fibre was perfomed, resulting in the deletion of all kinds of clearances between fibres. The scope of work, due to the nature of the material endurance, can be described as resilient. ***Figure 4.b*** shows the phase in which the fibres pass on the maximum value of force of 7.85 kN (maximum force values are given in ***Figure 5***). The machine jaws shifted by 8 mm. Figure 4c illustrates one of the last stages of the destruction of fibres. This is a phase in which the tensile strength of the beam decreases. The way of destroying the fibres makes individual fibres break and the force decreases appreciably. ***Figure 4.d*** shows the last fibres that have not been destroyed. The jaws of the machine moved 8.1 mm and the force dropped dramatically (***Figure 7***).

In order to facilitate interpretation of the results of the samples, markers were glued onto black-and-white chessboards. Thanks to these markers Tema 3.3 software, it was possible to accurately investigate the deformation of the sample

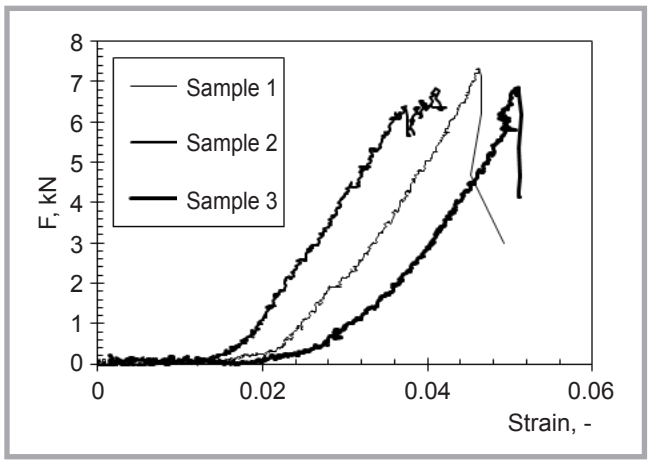

Figure 5. *Force curve characteristics as a function of the strain obtained from high speed recording – samples 1 - 3.*

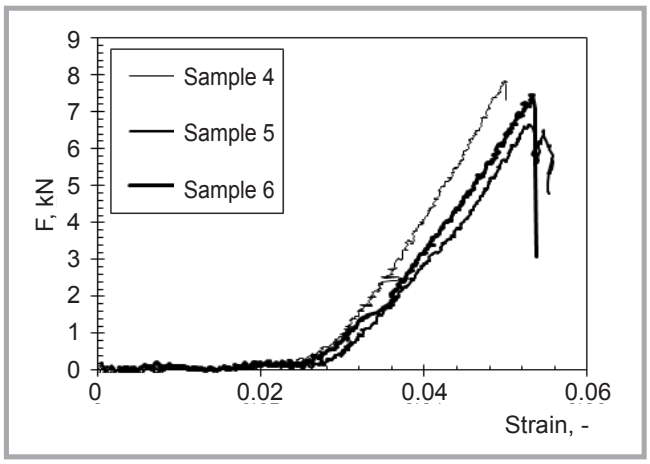

Figure 6. *Force curve characteristics as a function of the strain obtained from high speed recording – samples 4 - 6.*

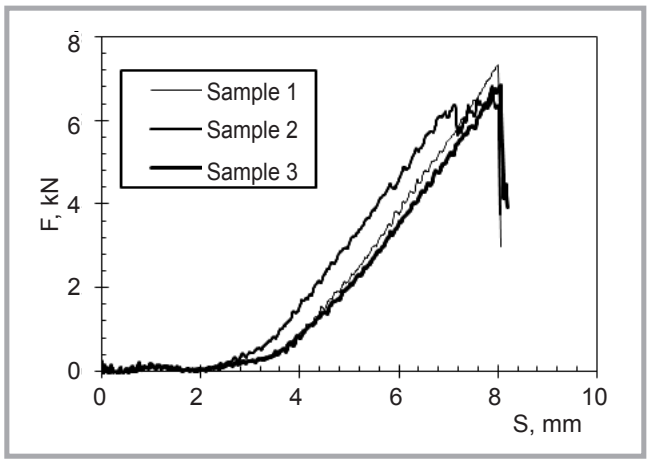

Figure 7. *Force curve characteristics as a function of displacement obtained from the Istron 8802 tensile machine – samples 1 - 3.*

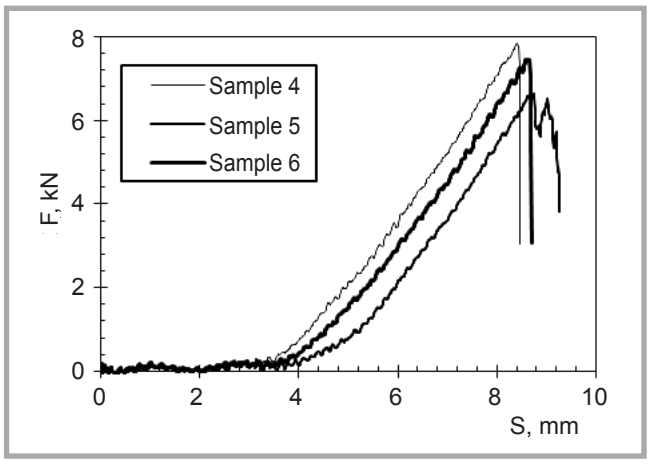

Figure 8. *Force curve characteristics as a function of displacement obtained from the Istron 8802 tensile machine – samples 4 - 6.*

by excluding the strain parts, which lay at the machine clamps. For the Tema 3.3 program the following values were defined:

- the location of the first marker along the sample;
- the location of the second marker along the sample;
- the distance between the markers was equal to 85 mm.

Elongation between the markers and their positions in the Tema 3.3 program had a resolution equal to 0.1 pixel.

$$X_{12} = X_2 - X_1 \tag{1}$$

$$\varepsilon_1 = \frac{X_{12} - X_{12}^0}{X_{12}^0} \tag{2}$$

where, X_{12}^0 initial distance between the markers, X_{12} - the distance between the markers at time t.

In ***Figures 5*** to ***8*** three main areas are clearly visible: In the first the force curves were almost horizontal, corresponding to the initial straightening of the fabric and a reduction in the clearances between individual fibres. In this area, aramid fibres and whole bundles were straightened under the influence of the displacement. The second area of the transition curve force corresponds to the moment where the roving bundles partially straightened and, in turn, began to carry the load. The force curve passes smoothly within the linear elastic scope of the bundles, lying close to each other and working uniformly. The destruction of the samples was recorded for a force in the range of 6.8 to 7.85 kN.

Numerical fabric modeling

In this chapter we will present an approach to model aramid special purpose fabric Twaron T750. The basic mechanical parameters for each bundle and fabric material were taken from the manufacturer's card. This information was used to fill the material card for the constitutive model of material describing the individual bundle.

Table 1. *Manufacturer's material card [16].*

Style	Linear density, dtexnom	Twaron-type	Weave	Set, per 10 cm		Set, per inch		Area density,		Thickness, mm	Minimum breaking strength, N/5 cm × 1.000		Minimum breaking strength, lb/in × 1.000	
	warp/weft	warp/weft		warp	weft	warp	weft	g/m²	oz/yd²		warp	weft	warp	weft
CT T750	3360f2000	2000	Plain	69	69	18	18	460	13.57	0.70	16.5	18.00	1.884	2.056

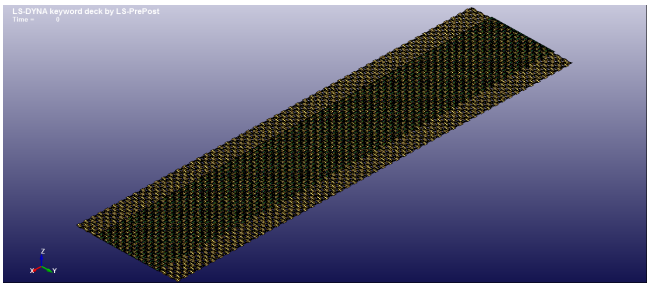

Figure 9. *Isometric view of the sample.*

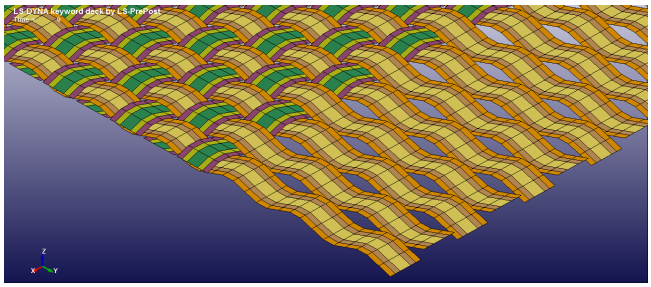

Figure 10. *View shows the architecture of the fabric.*

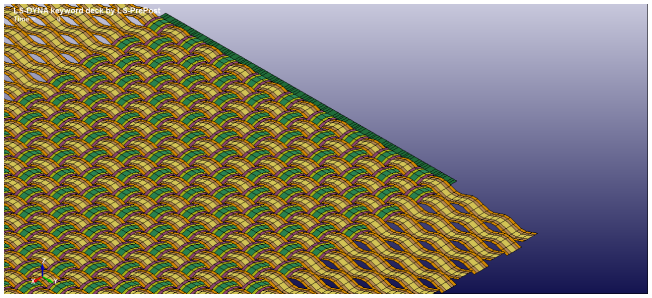

Figure 11. *Figure showing the edge of the sample modelled as a non-deformable body.*

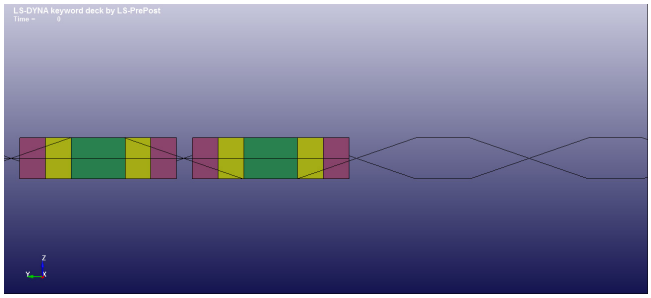

Figure 12. *Figure showing the view in the plane of the fabric.*

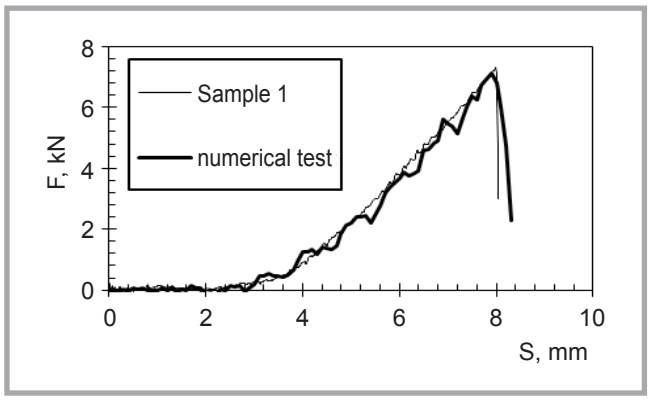

Figure 13. *The figure shows a comparison of the total force as a function of the displacement between the experiment and numerical studies.*

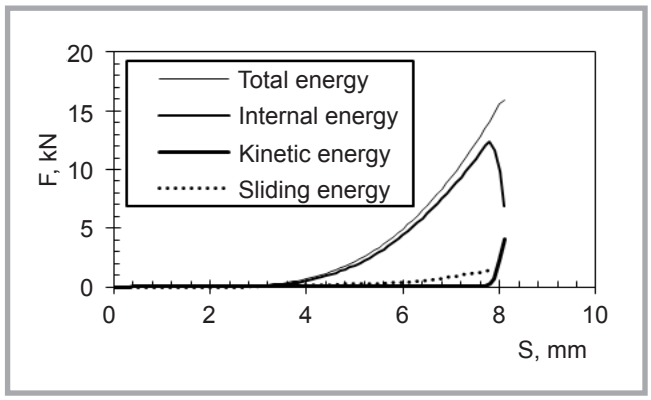

Figure 14. *Summary of the kinetic energy, internal energy, sliding energy and total energy of the sample.*

Numerical model description

The aforementioned experimental studies were used to validate the numerical model of the fabric in the aspect of its material and geometry. The research area of the sample was modelled accurately in terms of the shape and dimensions of each weave.

The choice of weave shape was modelled based on information from the manufacturer's material card as well as from the samples prepared.

The numerical experiments performed were used to study the phenomena occurring in the tensile fabric in the plane. It was therefore decided to model roving bundles using membrane elements. Each bundle is an individual object connected with other bundles only by contact definition. The contact definition used was CONTACT_AUTOMATIC_SURFACE_TO_SURFACE. In the contact card's variable thickness, the cross-section of the bundle was defined. This approach allowed the control of penetration at a constant elasticity of the roving bundles. The model was made based on 2D fully integrated membrane elements of constant thickness. Bundles in the direction of the samples were made of membrane elements, and those across the samples were with shell elements. The material model implemented to describe the bundles was MAT_PLASTIC_KINEMATIC. The material constants that were used in the card of the material were a Young's modululs equal to 57 GPa and a Poisson ratio of 0.001. Through the use of a very small Poisson number, stresses could separate in directions perpendicular to the bundle direction.

Figure 9 shows the whole research area of the sample modeled. The edge in the upper right corner of ***Figure 9*** (see also ***Figure 11***) had taken all the degrees of freedom. The opposite end of the sample in ***Figure 9*** (see also ***Figure 10***) was loaded by displacement with a speed equal to 10 m/s.

In ***Figure 11***, on the upper edge of the sample, a fully rigid body was modelled in order to fix the end of the sample. Such an approach to the modelling of the ends of the sample is consistent with the clamping of a sample of infinite rigid, in relation to the sample clamp of the testing machine

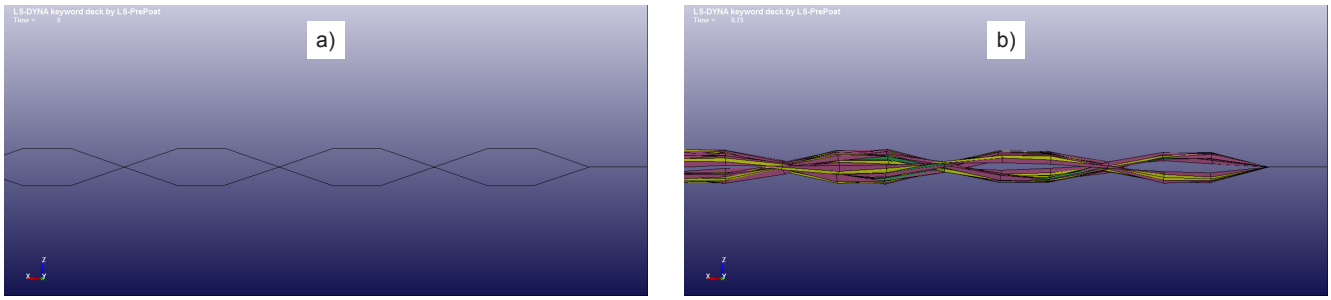

Figure 15. *a) unloaded roving bundle in the direction of the sample, b) the maximum of a stretched bundle at the time of sample breakages.*

Figure 12 shows a view in the plane of the sample with particular regard to the geometry of the bundle weave. The angle between the plane of the sample and the weave is about 20°.

Numerical test results

In this section, results of numerical experiments will be presented, performed using commercial LS-DYNA. The aim of the experiments was to match the force curve as a function of displacement obtained from the numerical analysis of the force curve obtained with the experimental data.

During the performance of experimental studies, special attention was paid to three things: Firstly the slope of the elastic curve was comparable to that of the force curve from the experiment. Secondly it was important that the modelled sample should break at a force in the range of 6.8 to 7.85 kN, which should also happen at a displacement in the range of 7.8 to 8.8 mm. The third element on which emphasis was placed was representation of the phenomenon of straightening the roving bundle and the transition to the elastic range.

As a result of adjusting the model of the samples, the graph displacement and longitudinal forces obtained acted on the sample. Results of the work are presented in ***Figure 13***. As an experimental model the first sample was selected . It is clearly visible that the general shape of the curve obtained from the numerical test corresponds to the graph obtained from the experiment. The uneven numerical curve is due to small dynamic phenomena such as the elastic wave moving in the medium of the bundle. Marginality dynamic effects in this issue will be addressed when discussing ***Figure 14***. The force error between the experiment and numerical is equal to 2.33%, and the displacement error 1.25%. One should notice that the numerical curve corresponds to the experimental curve during the straightening of fibres and in the transition to the elastic range.

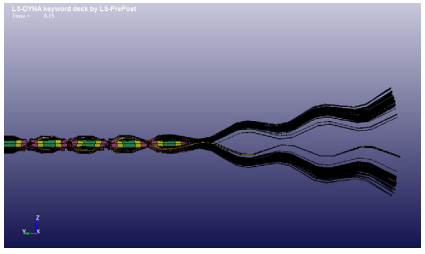

Figure 16. *An interesting effect of disperse the ends of the bundles arranged across the sample.*

In ***Figure 14*** is presented a summary of the kinds of energy to justify the increase in the movement speed in the numerical model of 200 times with respect to the experiment. The speed was increased for numerical reasons, namely to reduce the computation time to a reasonable level. In ***Figure 14*** it is clearly seen that the kinetic energy is a small part of the total energy of the model and is equal to about 18.55‰ (at the time of breaking of the sample).The potential energy is an 87.74% part of the total energy, while the sliding energy is 10.39% part of the total energy. In the opinion of the authors, it is a sufficient approximation of reality. In addition, thanks to the fully integrated elements used, the value of hour glassing energy was equal to zero.

Figure 15 shows the behaviour of the bundles under the influence of a load. In ***Figure 15.a***), we can see an unloaded bundle and in ***Figure 15.b***) - a bundle after maximum stretching. Clearly visible is the change in thickness of the fabric and that in the angle between the plane of the fabric and the weave. ***Figure 15.b***) shows that the bundles were brought into contact with each other and the entire fabric of the sample works in the elastic range.

In ***Figure 16*** we can see the interesting effect of the dispersal of the free ends of bundles arranged across the sample. This effect is caused by the tensioning and straightening of roving bundles in the direction of the sample. The behaviour of the free ends of the bundles coincide exactly with their behaviour in reality.

Conclusions

This article is an example of the effective combination of experimental and numerical investigations. Through a combination of these two approaches to the problem, we have created a faithful description of a complex phenomenon. It is important that there is an interaction effect between the roving bundles in the architecture of woven fabric on the behaviour of fabric in a global aspect. It has been proven that in the modelling of roving bundles in fabric using 2D elements shown here, the fabric is loaded in its plane correctly. In the article there is also presented an efficient way to study borderline quasi-static and dynamic phenomena. The next stage of research on special fabrics will attempt to develop a method of modeling fabric loaded perpendicular to its surface and compare the results with the experiment.

Acknowledgements

This study was supported by the National Centre for Research and Development Programme within the framework of INNOTECH in INNOTECH-K2/ IN2/56/182840/NCBR/13.

References

1. Penava Ž, Šimić Penava D, Knezić Ž. Determination of the Elastic Constants of Plain Woven Fabrics by a Tensile Test in Various Directions. *Fibres & Textiles in Eastern Europe* 2014; 22, 2(104): 57-63.
2. Hasani H, Planck H. Analysis of the Physical Fundamentals of an Objective

Integral Measuring System for the Determination of the Handle of Knitted Fabrics. *Fibres & Textiles in Eastern Europe* 2009; 17, 6(77): 70-75.
3. Stempień Z. Effect of Velocity of the Structure-dependent Tension Wave Propagation on Ballistic Performance of Aramid Woven Fabrics. *Fibres & Textiles in Eastern Europe* 2011; 19, 4(87): 74-80.
4. Szablewski P. Numerical Modelling of Geometrical Parameters of Textile Composites. *Fibres & Textiles in Eastern Europe* 2008; 6(71): 49–52.
5. Grechukhin AP, Seliverstov VY. Mathematical Model of Plain Weave Fabric at Various Stages of Formation. *Fibres & Textiles in Eastern Europe* 2014; 22, 5(107): 43-48.
6. Barauskas R. Multi-Scale Modelling of Textile Structures in Terminal Ballistics. In: *6th European LS-DYNA Users' Conference*, 2007.
7. Ha-Minh C, Imad A, Kanit T, Boussu F. Numerical analysis of a ballistic impact on textile fabric. *International Journal of Mechanical Sciences* 2013; 69: 32–39, doi:10.1016/j.ijmecsci.2013.01.014.
8. Nilakantan G, Keefe M, Gillespie JW Jr, Bogetti TA, Adkinson R. A Study of Material and Architectural Effects on the Impact Response of 2D and 3D Dry Textile Composites using LS-DYNA. In: *7th European LS-DYNA Users' Conference*, 2009.
9. Nilakantan G, Keefe M, Gillespie JW. Jr., Bogetti TA. Novel Multi-scale Modeling of Woven Fabric Composites for use in Impact Studies. In: *10th European LS-DYNA Users' Conference*, 2008.
10. Nilakantan G, Keefe M, Gillespie JW. Jr., Bogetti TA, Adkinson R, Wetzel ED. Using LS-DYNA to Computationally Assess the V_0-V_{100} Impact Response of Flexible Fabrics Through Probabilistic Methods. In: *11th European LS-DYNA Users' Conference*, 2010.
11. LS-DYNA, 2007, Keyword User Manual.
12. LS-DYNA, 2006, Teory Manual.
13. Zienkiewicz OC. Metoda Elementów Skończonych. Ed. Arkady, Warsaw, 1972.
14. Livermore Software Technology Corporation, Modelling of Composites in LS LS-DYNA.
15. Zacharski SE. Nonlinear mechanical behaviour of automotive air bag fabrics: an experimental and numerical investigation. The University of British Columbia, 2010.
16. Teijin Aramid, Ballistics material handbook, 2012.

Received 23.06.2014 Reviewed 06.02.2015